Master-Slave Coordination Using Virtual Constraints for a Redundant Dual-Arm Haptic Interface

Ghazaei Ardakani, Mahdi; Karlsson, Martin; Nilsson, Klas; Robertsson, Anders; Johansson, Rolf

Published in:
2018 IEEE/RSJ International Conference on Intelligent Robots and Systems (IROS)

DOI:
10.1109/IROS.2018.8594260

2018

Master-Slave Coordination Using Virtual Constraints for a Redundant Dual-Arm Haptic Interface*

M. Mahdi Ghazaei Ardakani[1], Martin Karlsson[2], Klas Nilsson[3], Anders Robertsson[2], and Rolf Johansson[2]

***Abstract*— Programming robots for tasks involving force interaction is difficult, since both the knowledge of the task and the dynamics of the robots are necessary. An immersive haptic interface for task demonstration is proposed, where the operator can sense and act through the robot. This is achieved by coupling two robotic systems with virtual constraints such that they have the same coordinates in the operational space disregarding a fixed offset. Limitations caused by the singular configurations or the reach of the robots are naturally reflected to either side as haptic feedback.**

I. Introduction

Everyday, more and more robots are employed to assist human workers for difficult and monotonous tasks. However, many tasks are still carried out manually, since it is overly difficult to program a robot to achieve a similar performance. Typically, these tasks involve interaction with an object or the environment, where the success of the task relies largely on the skills of the human. To program a robot, these skills need to be transferred to the robot. The most natural way for a human to do this is via demonstration [1]. However, robots do not have the same mechanical structure as the operator, which can create differences in the way that they can accomplish a task compared to the human. Hence, a lead-through programming interface for demonstrating a task can contribute by allowing the operator to perceive the differences and limitations of the robotic system during the actual demonstration.

Use of haptic feedback in teleoperation of robots [2] and in virtual reality [3] has been the subject of research for many years. Teleoperation with haptic feedback provides a suitable framework for immersive demonstration of a task. Utilizing both visual and haptic feedback from a robot or a model of it, an operator can ideally feel and perceive a task from the robot's perspective, hence enabling accurate demonstration including force specification.

Four-channel haptic systems are the most general form of haptic devices where both position and interaction forces are measured [4]. With the improved techniques to estimate joint torques and tool center point wrenches [5], [6], [7], many of the existing robot manipulators can be used as haptic devices without additional cost. Moreover, as dual-arm robots become popular, our idea is to utilize one of the arms as a convenient interface for demonstrating poses, trajectories, and forces for the other arm. A variety of experiments related to haptics and force estimation was carried out as reported in our earlier works [8], [9], [10], which was facilitated by the access to a prototype of YuMi robot with open control interfaces [11], [12] (See Fig. 1).

Fig. 1: A prototype of ABB YuMi Robot [13] as an example of dual-arm robots. Experiments for lead-through programming were carried out with this robot.

Several factors limit the transparency of a teleoperation system. In the one-dimensional linearized case, it is shown that the transparency and stability are conflicting requirements [14]. Delays are detrimental to both transparency and stability and have been studied widely [15], [16], [17]. However, in teaching [18] or virtual reality scenarios [3], they could be neglected. The transparency is further limited by the structures of the master or the slave devices. When two robotic systems are employed in a master-slave configuration, their workspace is limited to the points reachable by both systems simultaneously. This defines a common workspace for the robots. At the boundary of this common workspace, one or both of the systems are typically in a singular configuration with reduced manipulability. The transparency with respect to the environment is in fact contradictory with the desire to provide feedback concerning the limitations of a teleoperation system to the operator. The operator often expects haptic feedback associated with the presence of the robotic system, as long as it does not interfere much with the performance of the actual task.

In this paper we address coordination of master and slave nonlinear manipulators directly in task space. The need

*The research has received funding from the European Commission Horizon 2020 Framework Programme through the SOMA project (ICT645599), and from the VINNOVA project *Kirurgens Perspektiv*. The authors would like to thank Andreas Stolt, Cognibotics AB, for identifying the dynamics of the robot used in the experiments.

[1]The author is with the Department of Advanced Robotics (ADVR), Istituto Italiano di Tecnologia (IIT), Via Morego 30, 16163 Genoa, Italy. E–mail: mahdi.ghazaei@iit.it.

[2]The authors are with the Department of Automatic Control, LTH, Lund University, SE–221 00 Lund, Sweden and members of the LCCC Linnaeus Center and the ELLIIT Excellence Center at Lund University.

[3]The author is with the Department of Computer Science, LTH, Lund University, SE–221 00 Lund.

for reflecting the physical limitations of the teleoperation system to the operator becomes of major importance in several cases, e.g., when arbitrary robots are employed as haptic devices, the kinematics of master and slave robots are dissimilar, or similar master and slave devices are employed in different configurations. In case of the dual-arm YuMi robot, it is important to allow kinesthetic teaching in different configurations while demonstrating a task and to manage redundancy and singular configurations.

A. Previous Research

Currently, several approaches to mapping between a slave and a master device exist. A point-to-point kinematic mapping to maximize the common workspace and to reduce the effect of the deficient subspace was proposed in [19]. The problem of geometric correspondence was solved by adding proper offset and scaling [20], wherein the placement of the slave device was optimized to maximize the manipulability and the redundant degrees of freedom were mapped using the arm angles. A passive control law to precisely enforce coordination of nonlinear teleoperation in joint space was proposed in [21]. Attractive and repulsive potential fields have been used to introduce virtual constraint forces, which help the operator to keep the movements within a region of interest or to avoid singular configurations [22]. In virtual reality applications, some researchers have employed virtual spring-damper elements to penalize user motion along the direction resisted by the virtual mechanism [23].

The idea of a teleoperation system as a passive mechanical tool has been used by several researchers [24], [25]. In this paper, we also use a tool analogy to relate the motion of master and slave manipulators in task space. Knowing the physical properties of the tool, interaction forces by the environment and the force exerted by the human, the motion of the tool is uniquely determined. In this model, limitations of the tool are directly reflected to the operator since the dynamics of the tool has to always comply with the constraints. In our context, there is no distinction between the functionality of master and slave devices, e.g., the arms of a dual-arm robot, as both sides can be regarded as either master or slave.

B. Contribution

Defining a haptic mapping between two dissimilar manipulators, which could be interacted with at any point on their structures, is not trivial. This work proposes a flexible *constraint-based* approach to map between master and slave manipulators, which suits well for kinesthetic teaching. It relies on coupling between two *nonlinear* serial arms in *task space* on a *dynamical level*. This results in a mapping between two not-necessarily-similar arms, yet allowing a theoretically perfect pose tracking during free motion and perfect tracking of forces and torques in hard contact tasks of the end-effectors when there is no kinematic singularity. Specifically, it allows to use any 6-DOF or redundant robotic arm, mounted on any surface and with any initial position in a dual-arm haptic setup. Either of the arms can pass through singular configurations while the haptic feedback is being adjusted complying with restricted directions.

II. Control Principle

We consider in this section, a generic approach to mapping between a master and a slave manipulator while existing multibody dynamics are respected. The key idea to design the controller is to derive forces that are required to enforce desired virtual kinematic constraints. Controller synthesis via virtual constraints offers a great tool for control of different mechanical structures; see e.g. [26], [27], [28].

Let us assume that the dynamics of the manipulators are represented by the nonlinear system

$$\dot{x} = f(x) + g(x)u(x), \tag{1a}$$

$$y = h(x), \tag{1b}$$

where x, u, y denote the state vector, control signals and outputs, respectively. We define y as the deviation of the translation and orientation of a fixed frame on the slave arm from a fixed frame on the master arm plus a desired fixed offset. Without loss of generality, we choose these frames to be located at the end-effectors of the arms. We wish to find $u(x)$ that results in y being identically equal to zero and to find the zero dynamics of the system [29]. By zeroing the output, i.e., imposing the virtual constraint, we make sure that the end-effectors maintain the fixed offset.

A. Virtual Constraint

Assume that the robotic system has in total $n = n_1 + n_2$ degrees of freedom (DOF), where n_1 and n_2 are the DOF of the first and the second arm, respectively. Let us denote the generalized coordinates for both arms by $q \in \mathbb{R}^n$ and split it into the coordinates related to the first and the second arm according to $q := [q_1^T, q_2^T]^T$. The geometric constraint between two end-effectors can be expressed as

$$p_2 - p_1 = \Delta p, \tag{2a}$$

$$R_1^T R_2 = \Delta R. \tag{2b}$$

Here, the variables with subscripts 1 and 2 concern the first and the second arm, respectively. The position of each end-effector is denoted by $p_i \in \mathbb{R}^3$, and $R_i \in \mathrm{SO}(3)$ denotes the orientation, Δp and ΔR are the constant offsets in the position and the orientation, respectively. Based on Eq. (2), we define $e := [e_P^T, e_O^T]^T$, where $e_P = p_2 - (p_1 + \Delta p)$ and $e_O = \varepsilon$, as the vector part of the unit quaternion $\mathcal{Q} = \{\eta, \varepsilon\}$ corresponding to $R_2(R_1 \Delta R)^T$.

Theorem 1: The kinematic constraint corresponding to (2) can be rewritten as

$$G\dot{q} + g_0 = 0, \tag{3}$$

where $G = [-J_1, J_2] \in \mathbb{R}^{6\times n}$ and $g_0 = 0 \in \mathbb{R}^6$.

Proof: By differentiating the geometric constraints, we find the kinematic constraint. First, we multiply (2b) by R_1 from the left to obtain $R_2 = R_1 \Delta R$. Then, by differentiating both sides w.r.t. time, we find

$$S(\omega_2)R_2 = S(\omega_1)R_1\Delta R + 0 = S(\omega_1)R_2 \tag{4}$$

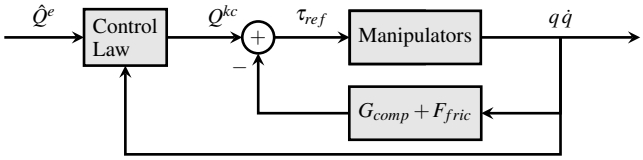

Fig. 2: Control scheme: estimated external torques $\hat{Q}^e$ and the states of the robots are inputs to the controller for the calculation of Q^{kc}, the forces due to kinematic constraints. The manipulators are gravity and Coulomb friction compensated.

Consequently,

$$S(\omega_2-\omega_1)R_2=0. \tag{5}$$

Here $S(\omega)$ is the skew-symmetric matrix corresponding to the vector product by the angular velocity ω. Therefore, fixed relative positions and orientations imply the following kinematic constraints

$$v_2-v_1=0, \tag{6a}$$
$$\omega_2-\omega_1=0, \tag{6b}$$

where $v_i=\mathrm{d}p_i/\mathrm{d}t$. By expressing these equations in the generalized coordinates, we find the differential kinematics relationships

$$J_{2P}(q_2)\dot{q}_2-J_{1P}(q_1)\dot{q}_1=0, \tag{7a}$$
$$J_{2O}(q_2)\dot{q}_2-J_{1O}(q_1)\dot{q}_1=0. \tag{7b}$$

Here $J_{iP}(.)$ and $J_{iO}(.)$ are the translational and rotational geometric Jacobians with respect to the end-effectors. Rewriting (7) in a matrix form completes the proof. ■

B. Dynamic Coupling

In this section, we find out the effect of the virtual constraint on the dynamics of the system. To derive the dynamics, we start off from the kinetic energy of the system

$$\mathscr{T}=\sum_i\frac{1}{2}m_i\dot{q}^T(J_P^i)^TJ_P^i\dot{q}+\sum_i\frac{1}{2}\dot{q}^T(J_O^j)^TR_{\ell_i}I_iR_{\ell_i}^TJ_O^i\dot{q}, \tag{8}$$

where m_i and I_i denote the mass and inertia matrix of link i, respectively, J_P^i and J_O^i denote partial Jacobians up to link i and R_{ℓ_i} is the rotation matrix of link i with respect to the world coordinate system. Since based on Fig. 2 we aim to compensate the gravitational forces, from the controller perspective there is no potential energy to be included in the Lagrangian $\mathscr{L}$. Accordingly, we have

$$\mathscr{L}=\mathscr{T}. \tag{9}$$

Assuming only viscous friction with coefficient μ_v, the equations of motion for the constrained system according to the Lagrange–d'Alembert theorem [30] can be derived as

$$M(q)\ddot{q}+C(q,\dot{q})\dot{q}=Q^e+Q^{kc}-\mu_v\dot{q}, \tag{10a}$$
$$G\dot{q}+g_0=0, \tag{10b}$$

where $M(q)$ is the mass matrix, $C(q,\dot{q})\dot{q}$ denotes the total effect of centripetal and Coriolis forces. The generalized external forces and the generalized forces due to the kinematic constraints are denoted by Q^e and Q^{kc}, respectively, and they fulfill the relations

$$Q^e=\tau+J^Th^e, \tag{11}$$
$$Q^{kc}=G^T\lambda, \tag{12}$$

where τ is the vector of external torques applied at the joints, h^e is the vector of forces and torques exerted on the end-effectors, and $\lambda(t,q,\dot{q})\in\mathbb{R}^6$ are Lagrange multipliers.

By introducing subscripts 1 and 2 for the parameters and variables, we find

$$M(q):=\mathrm{blkdiag}\left(B_1(q_1),B_2(q_2)\right), \tag{13}$$
$$J(q):=\mathrm{blkdiag}(J_1(q_1),J_2(q_2)), \tag{14}$$
$$C(q,\dot{q}):=\mathrm{blkdiag}\left(C_1(q_1,\dot{q}_1),C_2(q_2,\dot{q}_2)\right), \tag{15}$$
$$h^e:=\begin{bmatrix}h_1^e\\h_2^e\end{bmatrix},\ Q^{kc}:=\begin{bmatrix}Q_1^{kc}\\Q_2^{kc}\end{bmatrix}, \tag{16}$$

where the equations of motion for each individual arm is

$$B_i(q_i)\ddot{q}_i+C_i(q_i,\dot{q}_i)\dot{q}_i=\tau_i+J_i^T(q_i)h_i^e+Q_i^{kc}-\mu_v\dot{q}_i. \tag{17}$$

Therefore, the required torque to maintain the constraint is equal to the constraint force and for each arm derived as

$$Q_1^{kc}=-J_1^T(q_1)\lambda, \tag{18a}$$
$$Q_2^{kc}=J_2^T(q_2)\lambda. \tag{18b}$$

By introducing $x^T=\left(q^T,\dot{q}^T\right)$ and substituting λ with u, we can write (10) as

$$\dot{x}=\begin{bmatrix}\dot{q}\\M^{-1}(q)\left(-C(q,\dot{q})\dot{q}-\mu_v\dot{q}+Q^e+G^T(q)u\right)\end{bmatrix}$$
$$=:f(x)+g(x)u, \tag{19a}$$
$$\dot{y}=G(q)\dot{q}, \tag{19b}$$

where $M^{-1}=\mathrm{blkdiag}\left(B_1^{-1}(q_1),B_2^{-1}(q_2)\right)$. Equations (10)–(12) define a differential-algebraic equation system (DAE) of index 2, which can be solved numerically. From a control-design perspective, the solution is the zero dynamics of system (19) with relative degree two.

Let us define $\Gamma:=GM^{-1}G^T$. Considering the general results given in [29], the control $u^*(x)$ that makes the system invariant for all constant offsets can be calculated as

$$u^*=\Gamma^{-1}\left(GM^{-1}\left(C\dot{q}-\tau-J^Th^e+\mu_v\dot{q}\right)-\dot{G}\dot{q}\right), \tag{20}$$

where

$$\dot{G}:=\sum_{k=1}^{n}\left(\frac{\partial G}{\partial q_k}\dot{q}_k\right)=\left[-\dot{J}_1,\dot{J}_2\right]. \tag{21}$$

Furthermore, the zero dynamics are given by

$$M(q)\ddot{q}+W\left(C(q,\dot{q})\dot{q}-Q_e+\mu_v\dot{q}\right)+G^T\Gamma^{-1}\dot{G}\dot{q}=0, \tag{22}$$

where $W=I_{n\times n}-P$, and $P=G^T\Gamma^{-1}GM^{-1}$.

Theorem 2: Assume block diagonal matrices $K_p=\mathrm{blkdiag}\left(K_{tp},K_{op}\right)$ and $K_d=\mathrm{blkdiag}\left(K_{td},K_{od}\right)$ are positive definite. The state variable feedback

$$\lambda=u=u^*-\Gamma^{-1}\left(K_d\dot{y}+K_pe\right) \tag{23}$$

results in the asymptotic stability of (19).

Proof: Substituting the control law (23) in (19) results in the error dynamics

$$\ddot{y} + K_d \dot{y} + K_p e = 0. \tag{24}$$

Using the definitions of K_p and K_d, we get

$$\ddot{e}_P + K_{td}\dot{e}_P + K_{tp} e_P = 0, \tag{25a}$$

$$\dot{\tilde{\omega}} + K_{od}\tilde{\omega} + K_{op} e_O = 0, \tag{25b}$$

where $\tilde{\omega} = \omega_2 - \omega_1$.

The translational part (25a) is a linear system. Since K_{td} and K_{tp} are positive definite, it is exponentially stable. The stability of the rotational part (25b) can be established using the Lyapunov candidate function

$$V = \frac{1}{2}\tilde{\omega}^T K_{op}^{-1}\tilde{\omega} + (\eta_2 - \eta_1)^2 + (\varepsilon_2 - \varepsilon_1)^T(\varepsilon_2 - \varepsilon_1), \tag{26}$$

with the time derivative along the system trajectory

$$\dot{V} = -\tilde{\omega}^T K_{op}^{-1} K_{od}\tilde{\omega} \leq 0. \tag{27}$$

Invoking LaSalle's theorem [31], we conclude that $e_O = 0, \tilde{\omega} = 0$ is globally asymptotically stable. Therefore, for positive definite K_d and K_p, the solution of (24) converges asymptotically to zero. ∎

By substituting (23) into (18), we observe how the nonlinear feedback from both arms contributes to the control law. Assuming an accurate model of the arms and after gravity and Coulomb friction compensation, these control laws are applicable.

Note that whenever Γ is ill-conditioned, G is necessarily rank deficient. In this case, we can remove redundant constraints by assuming the forces perpendicular to the direction of relative motion being zero. This can be done by setting

$$\lambda = \tilde{G}\tilde{u}, \tag{28}$$

where $\tilde{G}$ is obtained by removing linearly dependent columns of G and $\tilde{u}$ is the new input signal. Accordingly, the same procedure for calculation of u applies to $\tilde{u}$ if we substitute G with $\tilde{G}^T G$.

Theorem 3: The equilibrium of system (10) is achieved when

$$\begin{aligned} h_2^e &\in \{-h_e + n \mid n \in \mathcal{N}(J_2^T)\}, \\ h_1^e &\in \{h_e + n \mid n \in \mathcal{N}(J_1^T)\}, \end{aligned} \tag{29}$$

where $h_e \in \mathbb{R}^6$ is an arbitrary wrench and $\mathcal{N}(\cdot)$ denotes the null space.

Proof: By setting the time derivatives in (10) to zero, the result is obtained. ∎

Corollary 1: If one of the arms is in a hard contact (standing still) and the configurations are not singular with respect to the end-effectors, that is J_i is full rank, the forces at the end-effectors are perfectly transferred, i.e., $h_2^e = -h_1^e$.

From (17) and the constraint forces (18), it is evident that λ plays the same role as the external wrenches h_i^e. Moreover, we conclude that λ can be interpreted as the cut forces as if the two arms were attached at their end-effectors.

The following theorem offers some simplifications in the special case of dual-arm robots.

Theorem 4: Assume that the only difference between the master and slave arms is the mounting planes. Then, excluding conservative forces (e.g., gravity), the dynamics of the arms has the same functional dependence on the joint coordinates, i.e.,

$$\tilde{B}(\mathfrak{q})\ddot{\mathfrak{q}} + \tilde{C}(\mathfrak{q}, \dot{\mathfrak{q}})\dot{\mathfrak{q}} = \tau, \tag{30}$$

where $\mathfrak{q} \in \mathbb{R}^{n/2}$ denotes the generalized coordinates of an arm.

Proof: Let R_0 denote the rotation of the mounting plane of arm 2 with respect to arm 1. By expressing Jacobians and moments of inertia in the rotated frame, we find

$$\begin{aligned} B_2(\mathfrak{q}) &= \sum_{i=1}^{n_2} \left(m_i J_{2P}^{(i)T} J_{2P}^{(i)} + J_{2O}^{(i)T} R_{\ell_i} I_i R_{\ell_i}^T J_{2O}^{(i)} \right) \\ &= \sum_{i=1}^{n_2} \left(m_i J_{1P}^{(i)T} R_0^T R_0 J_{1P}^{(i)} + J_{1O}^{(i)T} R_0^T \left(R_0 R_{\ell_i} I_i R_{\ell_i}^T R_0^T \right) R_0 J_{1O}^{(i)} \right) \\ &= \sum_{i=1}^{n_1} \left(m_i J_{1P}^{(i)T} J_{1P} + J_{1O}^{(i)T} R_{\ell_i} I_i R_{\ell_i}^T J_{1O}^{(i)} \right). \end{aligned} \tag{31}$$

This proves that $\tilde{B}(\mathfrak{q}) := B_1(\mathfrak{q}) = B_2(\mathfrak{q})$, hence $\tilde{C}(\mathfrak{q}, \dot{\mathfrak{q}}) := C_1(\mathfrak{q}, \dot{\mathfrak{q}}) = C_2(\mathfrak{q}, \dot{\mathfrak{q}})$, which completes the proof. ∎

C. Redundant Robots

Additional virtual constraints may be added for redundant robots. This allows impacting all the DOF from either side, not only those required for maintaining the offset between the end-effectors. In this subsection, we show specifically how constraints in the joint space as well as on relative distances can be introduced.

Assume H_i is a matrix, where each of its rows has exactly one non-zero element corresponding to a redundant joint. Consequently, we write a constraint in the joint space as

$$H_2 q_2 - H_1 q_1 = \Delta q, \tag{32}$$

where Δq is a constant vector. By taking the derivative of (32) w.r.t. time, we conclude

$$H_2 \dot{q}_2 - H_1 \dot{q}_1 = 0. \tag{33}$$

Now, augmenting this constraint to (3) results in

$$G = \begin{bmatrix} -J_1 & J_2 \\ -H_1 & H_2 \end{bmatrix}. \tag{34}$$

In the case of human-like robots, another approach can be to maintain the distance between the elbows. Assume $\Delta r := r_2 - r_1$ where r_i is the position vector of the elbow of the ith arm. Consequently, the constraint can be expressed using the 2-norm as $\|\Delta r\| = d \in \mathbb{R}$. By differentiation of $\|\Delta r\|^2 = d^2$ w.r.t. time, we find that

$$\Delta r \cdot \Delta v = 0, \tag{35}$$

where Δv is the relative velocity of the elbows. Rewriting (35) in terms of generalized coordinates results in

$$\begin{aligned} \Delta r \cdot \Delta v &= \Delta r^T (J_{2P}^{(e)} \dot{q}_2 - J_{1P}^{(e)} \dot{q}_1) \\ &= \Delta r^T \begin{bmatrix} -J_{1P}^{(e)} & J_{2P}^{(e)} \end{bmatrix} \dot{q} = 0, \end{aligned} \tag{36}$$

where $J_{iP}^{(e)}$ denotes the translational Jacobian w.r.t. the ith elbow. Therefore, the matrix G should be augmented according to

$$G = \begin{bmatrix} -J_1 & J_2 \\ -\Delta r^T J_{1P}^{(e)} & \Delta r^T J_{2P}^{(e)} \end{bmatrix}. \tag{37}$$

Based on the extended G in (34) or (37), a state feedback law similar to Eq. (23) can be designed.

III. Experiments

Simulations for the dual-arm industrial ABB YuMi [13] robot, with 7 joints per arm, are reported in [8]. For practical experiments, we used a prototype of ABB YuMi, which was equipped with the research interface ExtCtrl [11], [12]. The control algorithm in Sec. II was implemented on a PC, and communication with the internal controller of the robot was done through the research interface, at a sampling rate of 250 Hz. According to Fig. 2, the sum of the generalized forces from the kinematic constraints Q^{kc} and the gravity and the friction compensation signals, was sent as a torque reference to the internal robot controller. For the friction compensation at zero joint velocities, a dithering technique was utilized [10]. The worst-case scenario was experimentally evaluated, where the estimated external forces and torques were set to zero. Each tool flange of the robot was equipped with a force/torque sensor, and these were used for evaluation only. Further, the implementation was symmetric with respect to the arms, i.e., any arm could be used as master or slave, but we will refer to the arm currently grasped by a human as the master arm. The experimental setup is shown in Fig. 3. Additionally, a video that shows the setup and the experiments is available online [32].

Two different experiments were performed. In the first experiment, the left robot arm was used as master. First, free-space motion was conducted, in order to evaluate the motion tracking between the two arms. The right arm was then brought to collision with a concrete block in front of the robot, in order to evaluate force tracking and stability in contact with a stiff environment. When in contact the operator pushed the tool flange of the master arm in the positive y-direction, so that the slave arm was pushed against the block in order to excite the interaction forces. In the second experiment the right robot arm was used as master. Moving the master arm, the left arm was first brought to its upper reach limit. Thereafter, it was moved slightly to the side thus reaching the joint angle limit of joint 1, the joint closest to the body. The purpose of the second experiment was to evaluate stability properties and interaction forces when the slave arm reached internal physical limitations.

IV. Results

Data from the first experiment are shown in Fig. 4. It can be seen that motion tracking was achieved. The bottom plot compares the forces in the y-direction, as measured by the wrist-mounted force sensors. The force measured on the left arm has been negated for easier comparison, and corresponds to the interaction force experienced by the operator. After 50 s of free-space motion, a contact was established between

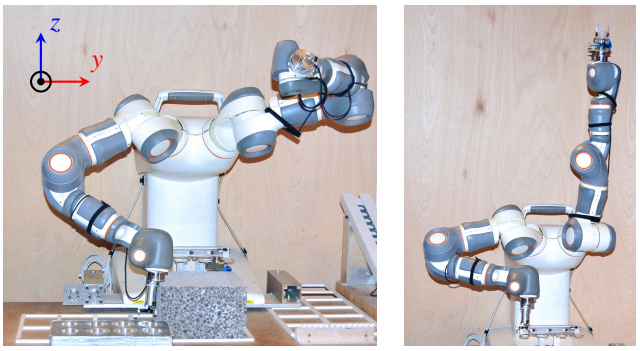

(a) (b)

Fig. 3: Robot configurations for experimental evaluation. In (a), the left arm of the robot was used as master, and the movement was such that the end-effector of the right arm established contact with the concrete block in front of the robot. In (b), the right robot arm was used as master, and the left arm was first brought upwards to its reach limit.

the right tool and the concrete block. It can be seen that force tracking was achieved, meaning that the operator experienced the contact forces as the slave arm. Moreover, the contact force from the concrete block prevented both arms from moving further in the y-direction, despite the force exerted by the operator. This behavior is the desired result of the virtual constraint.

Data from the second experiment are visualized in Fig. 5. The left arm was first brought to its upper reach limit. Despite a large force upwards exerted on the master arm by the operator, it can be seen that the master arm was prevented from moving in the z-direction by the virtual constraint. Joint 1 of the left arm was thereafter brought to its angle limit. Then, further motion of the arms in the limited direction was prevented despite pushing the master arm, since the joint limit of the slave arm was being propagated to the master arm thanks to the virtual constraint.

As expected from an impedance-type controller, stability was retained both during free-space motion, during contact with a stiff environment, and while reaching stiff internal limitations. In addtion, it can be concluded that the external physical limitation caused by the concrete block in the first experiment, had a similar effect as the internal limitations in the second experiment; the motion of the slave arm was limited directly, and the master arm was limited through the virtual constraint. Moreover, the virtual constraint transferred the contact forces between the arms, giving the operator the feeling of interacting with the environment using a tool.

V. Discussion

The proposed model for task demonstration solves the problem of capturing the interaction forces in addition to resolving the problem of correspondence between a human and a robot. Thanks to the separation of the operator–robot interface from the robot–workpiece interface, dual-arm lead-through programming (LTP) interface is more operator-friendly and less prone to unwanted demonstration side-

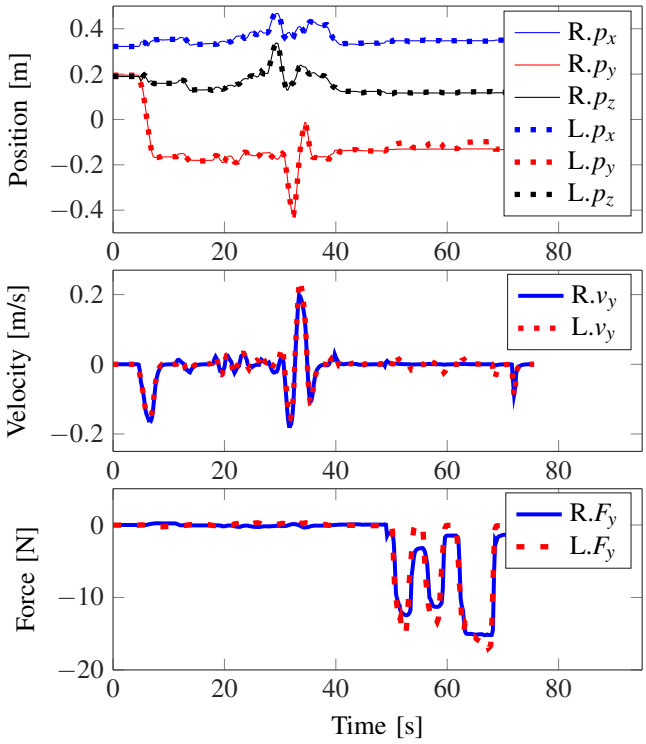

Fig. 4: Results from the first experiment. For an uncluttered view, only some of the dimensions are shown. The first plot from above shows the position of the arms, where position of the left arm has been compensated for with the desired offset between the arms. The second plot shows velocities in the y-direction, and the third plot shows forces in the y-direction.

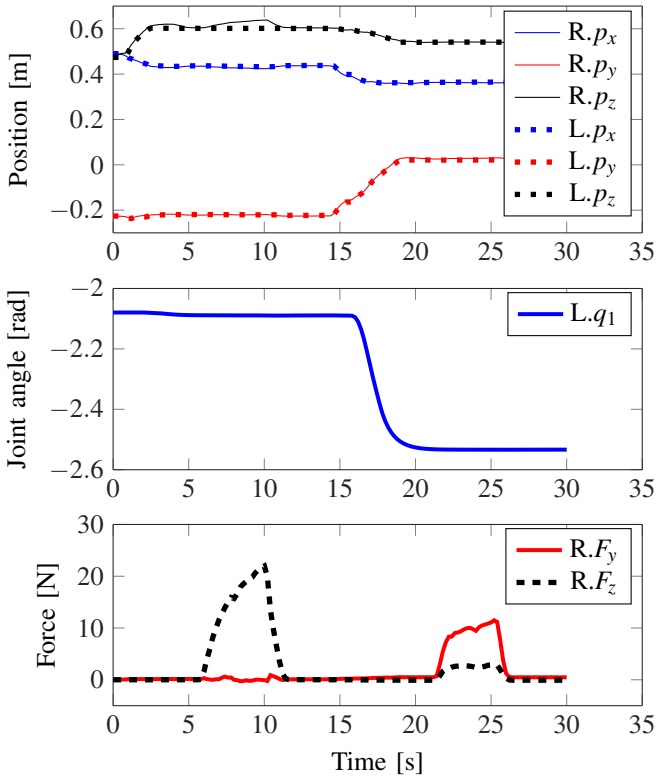

Fig. 5: Results from the second experiment. The master arm was subjected to large forces twice; first when the left arm reached a workspace limit in the z-direction, and thereafter when joint 1 of the left arm was in its lower angle limit.

effects compared to single-arm setups. Since the initial orientation and positions of the arms are free to be chosen, the operator has large flexibility for demonstration of a task from a convenient location with respect to the workpiece. The task-space mapping between manipulators by rendering the teleoperation system to behave as if the manipulators are physically attached, results in intuitive haptic feedback.

A major difficulty in using dissimilar robots for teleoperation is avoiding singularities. When a robot reaches a singular configuration, its controllability becomes limited. Consequently, one of the arms or both fail to follow a desired motion in Cartesian space. Using approaches such as iTaSC [33], [34] for defining purely kinematic constraints might lead to infeasible Cartesian motion due to the limitations of one or both robots. A common approach to deal with the calculation of velocities at singular configurations is to use damped pseudo-inverse [35]. However, this does not guarantee stability of the system and proper haptic feedback to the operator. On the other hand using the proposed virtual constraint approach, kinematic constraints in singular configurations influence both arms via a dynamic coupling and the motion remains always compatible with the constraints.

By including the dynamics according to our approach, as long as constraint forces remain bounded, the motion will comply with the kinematic constraints. This way the kinematic constraints are naturally integrated into the calculation of the motion while their feasibility can also be quantified. A possible drawback of the proposed approach, however, is that existing dynamical properties of the robots may be undesired. This problem can be circumvented by using local feedback to adjust the apparent physical properties of manipulators, before the application of the proposed controller according to Fig. 2.

Cooperative manipulation despite having a different objective shares a similar motion constraint in task space, i.e., the relative position and orientation of the robots are fixed [36]. Accordingly, similar control laws can be used in the context of haptic interface. With respect to the position error, our approach addresses redundant as well as non-redundant robots and can easily be extended to allow for various constraints.

To reduce the loads on the joint limits, a joint constraint can be activated as soon as the limit is reached and relaxed whenever the constraint forces are in the same direction as the constraints. Moreover, task related forces such as those required to limit the motion to a certain plane or along a certain line can be derived using the same approach discussed in this article. Coupling between other points than the actual end-effectors, locking certain joint angles or Cartesian directions, and scaling can also be introduced to create a variety of motions.

VI. Conclusion

A haptic interface for task demonstration using two redundant manipulators has been introduced, where interaction with any point of the arms is allowed. We have used a tool analogy for designing the haptic interface such that restrictions in the mechanism are naturally reflected to the operator as haptic feedback. Specifically, we derive a control law coupling the motion of two nonlinear robotic arms in task space. This approach is based on introducing virtual constraints between the multibody models of the arms, ensuring that the velocities of the end-effectors remain identical. Using this formalism, robots with different kinematics can be employed and they can pass through singular configurations while the haptic feedback is adjusted accordingly. Additional constraints between master and slave manipulators for redundant robots or joint limits can easily be included. Our approach leads to an immersive haptic interface, which allows the operator to generate trajectories reproducible by the robot in an intuitive way. A video illustrating the functionality of the system is available online [32].

References

[1] S. H. Lee, I. H. Suh, S. Calinon, and R. Johansson, "Autonomous framework for segmenting robot trajectories of manipulation task," *Autonomous robots*, vol. 38, no. 2, pp. 107–141, 2015.

[2] P. F. Hokayem and M. W. Spong, "Bilateral teleoperation: An historical survey," *Automatica*, vol. 42, no. 12, pp. 2035–2057, 2006.

[3] D. Constantinescu, "The feel of virtual mechanisms," in *Product Engineering*. Springer Netherlands, 2008, pp. 231–242.

[4] I. Aliaga, A. Rubio, and E. Sanchez, "Experimental quantitative comparison of different control architectures for master-slave teleoperation," *IEEE Trans. Control Systems Technology*, vol. 12, no. 1, pp. 2–11, 2004.

[5] A. Wahrburg, S. Zeiss, B. Matthias, and H. Ding, "Contact force estimation for robotic assembly using motor torques," in *Proc. IEEE Int. Conf. Auto. Sci. Eng. (CASE)*, 2014, pp. 1252–1257.

[6] A. Stolt, A. Robertsson, and R. Johansson, "Robotic force estimation using dithering to decrease the low velocity friction uncertainties," in *Proc. IEEE Int. Conf. Rob. Auto. (ICRA)*, 2015, pp. 3896–3902.

[7] M. Linderoth, A. Stolt, A. Robertsson, and R. Johansson, "Robotic force estimation using motor torques and modeling of low velocity friction disturbances," in *Proc. IEEE/RSJ Int. Conf. Intell. Rob. Sys. (IROS)*, Tokyo, Japan, 2013, pp. 3550–3556.

[8] M. M. Ghazaei Ardakani, "On trajectory generation for robots," PhD Thesis, Department of Automatic Control, Lund University, Lund, Sweden, Dec. 2016, Thesis No. TFRT--1116--SE.

[9] A. Stolt, F. B. Carlson, M. M. Ghazaei Ardakani, I. Lundberg, A. Robertsson, and R. Johansson, "Sensorless friction-compensated passive lead-through programming for industrial robots," in *Proc. IEEE/RSJ Int. Conf. Intell. Rob. Sys. (IROS)*, Hamburg, Germany, 2015, pp. 3530–3537.

[10] M. Capurso, M. M. Ghazaei Ardakani, R. Johansson, A. Robertsson, and P. Rocco, "Sensorless kinesthetic teaching of robotic manipulators assisted by observer-based force control," in *Proc. IEEE Int. Conf. Rob. Autom. (ICRA)*, Singapore, May 29–3 June 2017, pp. 945–950.

[11] A. Blomdell, G. Bolmsjö, T. Brogårdh, P. Cederberg, M. Isaksson, R. Johansson, M. Haage, K. Nilsson, M. Olsson, T. Olsson, A. Robertsson, and J. Wang, "Extending an industrial robot controller–Implementation and applications of a fast open sensor interface," *IEEE Robotics & Automation Magazine*, vol. 12, no. 3, pp. 85–94, 9 2005.

[12] A. Blomdell, I. Dressler, K. Nilsson, and A. Robertsson, "Flexible application development and high-performance motion control based on external sensing and reconfiguration of ABB industrial robot controllers," in *Proc. Workshop "Innovative Robot Control Architectures for Demanding (Research) Applications—How to Modify and Enhance Commercial Controllers", IEEE Int. Conf. Rob. Autom. (ICRA)*, Anchorage, AK, June 2010, pp. 62–66.

[13] ABB Robotics, "YuMi product page," http://www.abb.com/yumi, accessed: 2015-01-15.

[14] D. Lawrence, "Stability and transparency in bilateral teleoperation," *IEEE Trans. Rob. Autom.*, vol. 9, no. 5, pp. 624–637, 1993.

[15] R. Anderson and M. Spong, "Bilateral control of teleoperators with time delay," *IEEE Trans. Automatic Control*, vol. 34, no. 5, pp. 494–501, 1989.

[16] D. Lee and M. Spong, "Passive bilateral teleoperation with constant time delay," *IEEE Trans. Robotics*, vol. 22, no. 2, pp. 269–281, 2006.

[17] T. Hatanaka, N. Chopra, and M. W. Spong, "Passivity-based control of robots: Historical perspective and contemporary issues," in *Proc. 54th IEEE Conf. Decision and Control (CDC)*, Osaka, Japan, 2015, pp. 2450–2452.

[18] M. M. Ghazaei Ardakani, J. H. Cho, R. Johansson, and A. Robertsson, "Trajectory generation for assembly tasks via bilateral teleoperation," in *Proc. 19th IFAC World Congress*, vol. 19, no. 1, Cape Town, South Africa, 8 2014, pp. 10 230–10 235.

[19] Y. Chen, J. Zhang, C. Yang, and B. Niu, "The workspace mapping with deficient-DOF space for the PUMA 560 robot and its exoskeleton arm by using orthogonal experiment design method," *Rob. and Computer-Integrated Manufacturing*, vol. 23, no. 4, pp. 478–487, 2007.

[20] J. Rebelo and A. Schiele, "Master-slave mapping and slave base placement optimization for intuitive and kinematically robust direct teleoperation," in *Proc. 12th Int. Conf. Control, Automation and Systems (ICCAS)*, Jeju Island, Korea, 2012, pp. 2017–2022.

[21] D. Lee and P. Y. Li, "Passive bilateral control and tool dynamics rendering for nonlinear mechanical teleoperators," *IEEE Trans. Robotics*, vol. 21, no. 5, pp. 936–951, 2005.

[22] N. Turro, O. Khatib, and E. Coste-Maniere, "Haptically augmented teleoperation," in *Proc. IEEE Int. Conf. Rob. Autom. (ICRA)*, Seoul, Korea, May 21–26 2001, pp. 386–392.

[23] D. Constantinescu, S. E. Salcudean, and E. A. Croft, "Haptic manipulation of serial-chain virtual mechanisms," *J. Dynamic Systems, Measurement, and Control*, vol. 128, no. 1, pp. 65–74, 2006.

[24] T. Itoh, K. Kosuge, and T. Fukuda, "Human-machine cooperative telemanipulation with motion and force scaling using task-oriented virtual tool dynamics," *IEEE Trans. Rob. Auto.*, vol. 16, no. 5, pp. 505–516, 2000.

[25] D. Lee and P. Y. Li, "Passive bilateral feedforward control of linear dynamically similar teleoperated manipulators," *IEEE Trans. Rob. Auto.*, vol. 19, no. 3, pp. 443–456, 2003.

[26] L. Freidovich, A. Robertsson, A. Shiriaev, and R. Johansson, "Periodic motions of the pendubot via virtual holonomic constraints: Theory and experiments," *Automatica*, vol. 44, no. 3, pp. 785–791, 2008.

[27] A. S. Shiriaev, L. B. Freidovich, A. Robertsson, R. Johansson, and A. Sandberg, "Virtual-holonomic-constraints-based design of stable oscillations of Furuta pendulum: Theory and experiments," *IEEE Trans. Robotics*, vol. 23, no. 4, pp. 827–832, 2007.

[28] E. R. Westervelt, J. W. Grizzle, C. Chevallereau, J. H. Choi, and B. Morris, *Feedback Control of Dynamic Bipedal Robot Locomotion*. Boca Raton: CRC press, 2007.

[29] A. Isidori, *Nonlinear control systems*, 3rd ed. London: Springer-Verlag, 1995, ch. 5.

[30] A. M. Bloch, *Nonholonomic mechanics and control*. New York: Springer Science & Business Media, 2003.

[31] H. K. Khalil, *Noninear Systems*. Prentice-Hall, New Jersey, 1996.

[32] M. M. Ghazaei Ardakani, M. Karlsson, K. Nilsson, A. Robertsson, and R. Johansson. (2018) Master-slave coordination using virtual constraints for a redundant dual-arm haptic interface. Dept. Automatic Control, Lund University. [Online]. Available: https://www.youtube.com/watch?v=4u57bEA4bqg

[33] G. Borghesan, B. Willaert, T. De Laet, and J. De Schutter, "Teleoperation in presence of uncertainties: a constraint-based approach," in *Proc. 10th IFAC Symposium on Robot Control*, 2012, pp. 385–392.

[34] G. Borghesan, B. Willaert, and J. De Schutter, "A constraint-based programming approach to physical human-robot interaction," in *Proc. IEEE Int. Conf. Rob. Autom. (ICRA)*, 2012, pp. 3890–3896.

[35] A. S. Deo and I. D. Walker, "Overview of damped least-squares methods for inverse kinematics of robot manipulators," *Journal of Intelligent and Robotic Systems*, vol. 14, no. 1, pp. 43–68, 1995.

[36] M. Uchiyama and P. Dauchez, "A symmetric hybrid position/force control scheme for the coordination of two robots," in *Proc. IEEE Int. Conf. Rob. Autom. (ICRA)*, Philadelphia, 1988, pp. 350–356.